Caving 2022 - Y Potvin (ed.)

doi:10.36487/ACG_repo/2205_14

Geotechnical analysis and ground support selection for the Oyu Tolgoi Crusher Chamber #2

GB Sharrock *Itasca Australia Pty Ltd, Australia*

J Ooi *Rio Tinto, Australia*

B Baasanjav *Oyu Tolgoi LLC, Mongolia*

Abstract

Oyu Tolgoi (OT), in the South Gobi region of Mongolia, is one of the largest known copper and gold deposits in the world. At peak production, Oyu Tolgoi is expected to produce 500,000 tonnes per annum of copper. The Panel 2 (PC2) crusher is a key component of the OT underground ore handling system, which has a total capacity of 95 ktpd; the PC2 crusher processes 45 ktpd of this total. The PC2 crusher chamber is a large excavation located at a depth of 1,300 m, with a stand-off distance of 280 m from the Panel 2 footprint. This paper describes the geomechanical analyses and design carried out to evaluate stability and support of the chamber including:

- *Overview of chamber geometry and location, a literature review and benchmarking study.*
- *Site characterisation and derivation of material properties.*
- *Numerical and analytical modelling for estimation of excavation stability and deformation.*
- *Ground support and reinforcement selection.*

Keywords: *large chamber, deep and high stress mining, ground support, numerical modelling*

1 Overview of chamber design

1.1 Location, geometry, sequence, cave stand-off distance

In the South Gobi region of Mongolia, Oyu Tolgoi (OT) is one of the world's largest known copper and gold porphyry deposits, situated approximately 550 km south of the capital, Ulaanbaatar, and 80 km north of the Mongolia–China border). OT is jointly owned by the Government of Mongolia, which has 34% ownership, and Turquoise Hill Resources, which owns 66%. Rio Tinto owns 50.8% of Turquoise Hill Resources and provides extensive and critical management services and support to the project. More detail on the OT project can be found in Ooi et al. (2022).

At the time of publication, the first lift (Hugo Lift) is still under development. The current design comprises three block caves (Panels 0, 1 and 2, Figure 1). The PC2 crusher services Panel 2, and is located 280 m from Panel 2, at a depth of 1,300 m.

Key considerations for design of the chamber development sequence and ground support include:

- Excavation sequence: Design a development sequence and support system, with suitable factors of safety, to provide safe development of the chamber. A top-down excavation sequence (Figure 1) was selected to eliminate the need for overhand mining, and to facilitate installation of support and minimise the potential for instability.
- Lifecycle stability: A key design consideration is evaluation of lifecycle stress and deformation changes to the chamber complex, and associated mobilisation of geological structures, induced by the mining of the three caves (e.g. Figure 1, West Bat Fault).

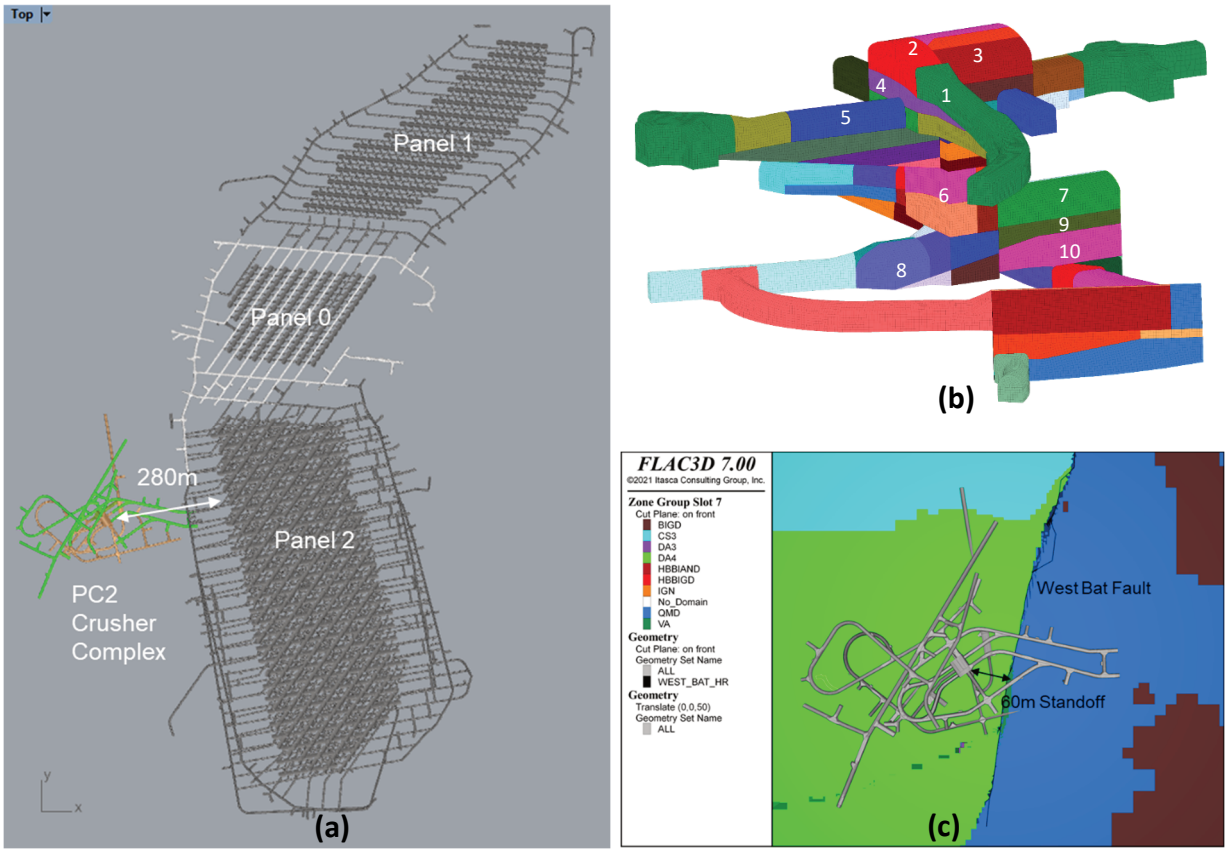

Figure 1 (a) Plan view: PC2 crusher chamber stand-off distance from Panel 2 cave; (b) Chamber development sequence (simplified) – FLAC3D model; (c) Plan view: crusher complex in proximity of West Bat Fault

Chamber dimensions and design aspects relevant to the current study are as follows:

- Chamber dimensions (Figure 2). The minimum span of the upper chamber is around 21 m, and the long total length of the lower chamber is more than 50 m.
- Pillar dimensions (Figure 2): Pillars are formed between the upper (Figure 3) and lower chambers, on the south and north ends of the main chambers (aspect ratios of 1.3 and 1.5 respectively).

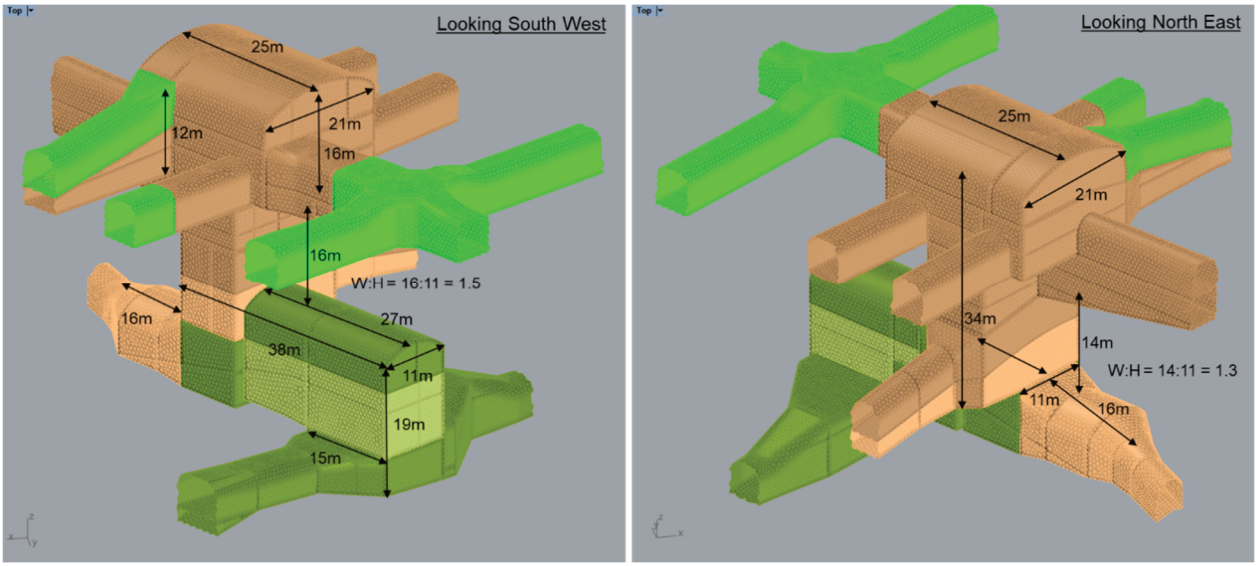

Figure 2 PC2 crusher chamber dimensions

Figure 3 Looking northwest during development of the chamber

1.2 Design considerations and methodology

Key considerations for the PC2 Chamber complex identified during the study included: structural wedges/damage, brittle damage and convergence, rock bursting during construction of the chamber, lifecycle stability and cave interaction dynamics, 60 m proximity to an unconformity bounded by a major regional fault which intersects the Panel 2 cave.

Keys aspects of the design methodology are described below with reference to three separate stages of the chamber lifecycle:

1. Greenfields design based on drillhole data:
    a. Data collection: Intact strength and deformability, structure, joints, rock mass classification.
    b. Analytical methods: Kinematic analysis, analysis of faults.
    c. Cave shapes: Numerical calculation of cave shapes based on mine production schedule using coupled FLAC3D–CAVESIM models or CAVESIM–CAP program.
    d. Preliminary modelling: (FLAC3D or 3DEC) to assess of depth of damage and excavation convergence, utilising support pressure embedded in larger model including cave shapes and sequence, and explicit structure. Analysis of faults/movement mechanisms.
    e. Ground support design: Analytical/empirical/kinematic assessment of ground support required based on numerical depth of damage with a Factor of Safety of 1.5 applied to all load and deformation calculations; bolt type and spacing are selected to satisfy constructability and durability.
    f. Detailed modelling: (FLAC3D or 3DEC) Detailed numerical modelling incorporating explicit support and reinforcement.

2. During chamber development:
    a. Instrumentation to monitor support loads (smart cables) and deformation (extensometers and convergence).
    b. Face mapping to reduce geotechnical uncertainty and understand structures.
    c. Numerical back-analysis to validate assumptions and inputs using observational data.
    d. Update empirical/kinematic/analytical analysis and ground support.
3. During cave operation:
    a. Ongoing monitoring of support loads, fibre-reinforced shotcrete (FRS) response, and deformation (extensometers, convergence pins, etc).
    b. Additional analytical and numerical modelling to recalibrate assumptions and support performance.

1.3 Ground support design

The ground support and reinforcement system selected for the PC2 Chamber is designed to withstand static and dynamic demand, and is described as follows with reference to Table 1, and Figure 4:

The ground support design and installation sequence for the crusher chamber is as follows:

1. Apply 1st layer of FRS, 35MPa, 350 J @ 40 mm displacement, 50 mm thickness.
2. Install woven mesh, 10 mm wire, pinned by 3 m resin bolts at 1 × 1 m bolt spacing.
3. Apply 2nd layer of fibrecrete to cover woven mesh (35 MPa, 350 J @ 40 mm displacement, 50 mm thickness).
4. Install welded mesh, 4 mm wire, pinned by 2.4 m length dynamic resin bolts and 21.8 mm debonded cable bolts (backs and walls: 14 and 10 m, 1.4 × 1.4 m dice five pattern) – Figure 4.

Based on analytical calculations, the rockbolt and cable bolt system were found to have a minimum static Factor of Safety (FS) of 1.5. Numerical estimates based on S-Curve assumptions indicate static factors of safety greater than 2.1 across the lifecycle of the chamber. Figure 4 shows final support installed partway through construction of the upper chamber.

Table 1 Reinforcement Capacity for OT PC2 Chamber

Bolt type	Ultimate tensile strength (kN)^	Yield strength (kN)^	Static elongation (%)^	Maximum dynamic displacement (mm)#	Maximum dissipated energy (kJ)#	Bolt spacing (m)	Bolt length (m)
25 mm resin bolt (J-Tech)	260	215	15	174	48	1 × 1	3
23 mm dynamic bolt (Yield-Lok)	267	200	7	565	67	1 × 1	2.4
17.8 mm 7-wire cable bolt (Secta)	350	280	3.5	105	31	2 × 2	10
21.8 mm cable bolt (Superstrand)*	590	525	5	–	–	2 × 2	14

Note: * The 21.8 mm cable bolt has 2 m debonded sleeve, 1 m from toe. ^ Static capacity is based on Jennmar's catalogue. # Dynamic capacity based on test results obtained from momentum transfer Western Australian School of Mines method (Player et al. 2008).

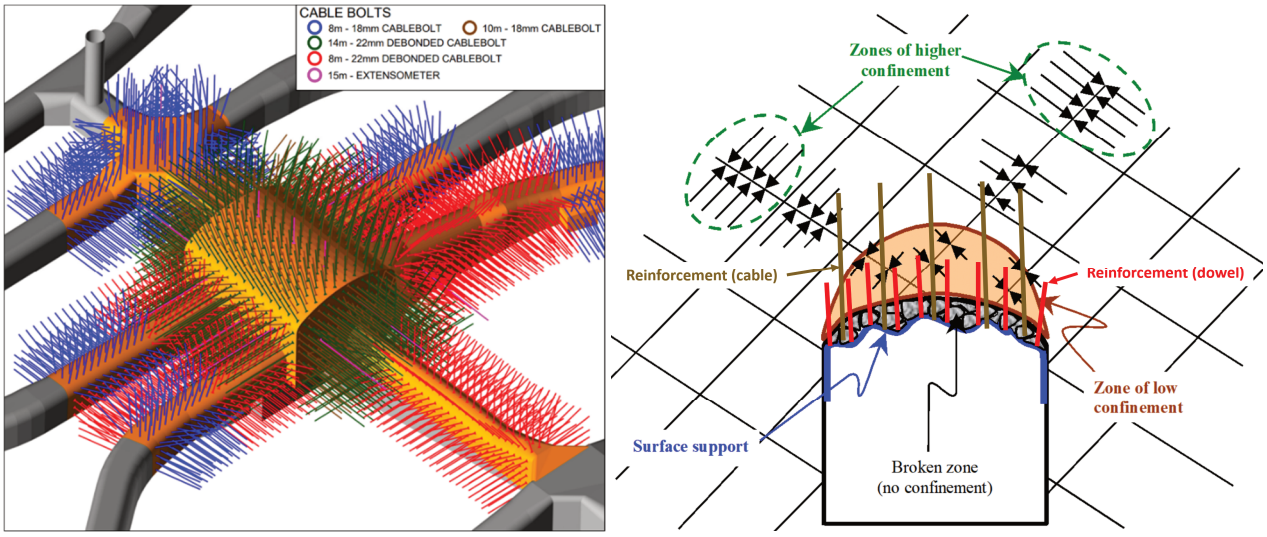

Figure 4 (a) Cable bolting design for PC2 Chamber; (b) Illustration of the underground excavation and the role of ground support in response to different regions of confinement stress

1.4 Benchmark

A benchmarking study to establish recent ground support practices was undertaken across 12 caving and stoping operations including El Teniente (Hormazabal et al. 2014), Ernest Henry (Campbell et al. 2013), Finsch (Talu & Wilson 2004), Cadia (Earl 2009), Freeport (Casten et al. 2000), Henderson (Callahan et al. 2000), and Civil Chambers (Hönisch 1988; Hoek 2001). Benchmarking considered the ground conditions, chamber dimensions, depth, in situ stress, stand-off distance to excavations, and ground support system.

The benchmarking study showed that:

- Design methodology: Support and reinforcement is designed using a hybrid approach of analytical and numerical methods as described in Section 1.2.
- Ground response: In high stress conditions, several case studies exist for chambers located too close to operating caves, resulting in static damage and/or damage to support. During chamber development in high strength rock, bursting has occurred in pillar geometries in chambers and bins.
- Primary reinforcement: Resin grouted rockbolts, 2 to 4 m in length and between 20 and 35 mm in diameter.
- Secondary reinforcement: Cable bolts, 4 to 14 m in length based on span and estimated depth of damage. Debonded cables were used in some chambers where high deformations or dynamic loads were expected.
- Support: FRS thickness between 100 and 200 mm and weld mesh. Some operations install mesh between FRS layers. If high deformations are expected, operations install mesh over the FRS layer.

2 Geomechanical environment

2.1 Domains and faults

The majority of the PC2 area including the chamber is located within the Devonian DA4 unit (Figure 1) which consists of basaltic flow and basaltic tuff breccia with some interbedded volcanic sandstone. DA4 units are clearly identified with their colour, texture and carbonate veining. Only the most eastern part of the design is likely to be in quartz monzodiorite which contacts with the DA4 unit along the West Bat Fault. The crusher model was embedded within a larger mine scale model incorporating a large number of structures modelled

using interfaces (Figure 5). Interfaces in FLAC3D have no thickness and are characterised by Coulomb sliding and/or tensile and shear bonding. Conservative shear strength properties have been adopted for all the faults (Figure 5).

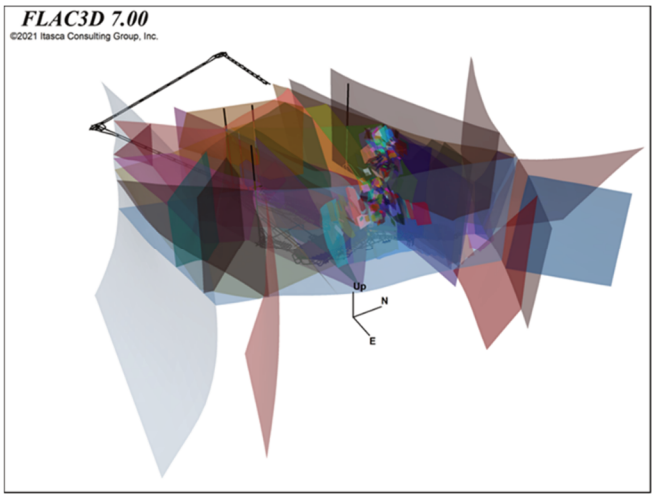

Strength parameters for the explicit faults.

Property	Value
Cohesion (Pa)	0
Friction angle (°)	25
Tensile strength (Pa)	0
Dilation Angle (°)	0

Figure 5 FLAC3D mine scale model incorporating explicit structures

2.2 Rock mass classification, intact and rock mass strength

Rock mass classification: The rock mass has a high geological strength index (GSI) with a very low fracture density. GSI was estimated via RMR_{89} (Hoek 2007). The mean logged RMR_{89} is 79, and GSI is 74. Figure 6 shows the statistical distribution of logged RMR_{89}.

Intact strength: The intact uniaxial compressive strength (UCS) is around 90 MPa; lower and upper bound m_i values are 18 and 29 respectively.

Rock mass strength:

Two approaches were assessed, with strength enveloped shown in Figure 7:

- Hoek–Brown GSI (HB–GSI) method of Hoek & Brown (2019); according to brittle theory HB–GSI is applicable to GSI <65–70. Even so, many modellers still use HB–GSI for high GSI materials as it is more conservative than S-Curve. Also, the S-Curve is new and relies on difficult to measure intact parameters such as crack initiation stress and mi. HB–GSI gives rock mass compressive strength, UCS_{RM} ≈ 20 MPa, mb ≈ 7-12, indicating a strong, competent rock mass (core images: Figure 7).
- Brittle (S-Curve) approach of Kaiser et el. (2015) and Bewick (2021); applicable to GSI >=70. S-Curve compressive strength is UCS_{RM} ≈ 30 MPa, mb ≈ 34.

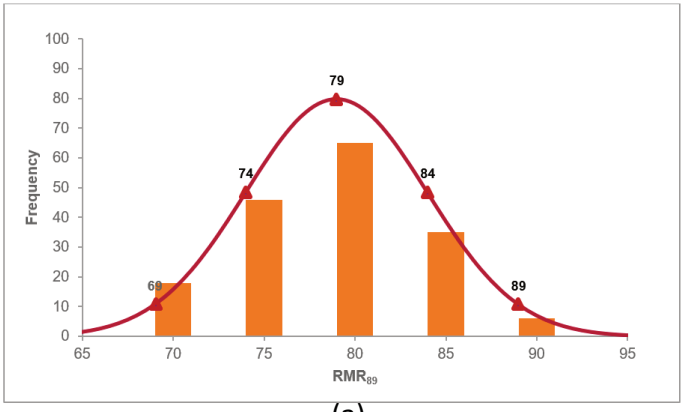

(a)

Strength Parameter		Value
Hoek-Brown Classification	σ_{ci} (MPa)	88.64
	m_i	29.46
	GSI	74
	D	0
	E_i (GPa)	66.95
	ν_i	0.2145
Hoek-Brown Criterion	m_b	11.641
	a	0.501
	s	0.0556
Rock Mass Parameters	σ_{cm} (MPa)	42.93
	σ_c (MPa)	20.85
	E_{rm} (GPa)	53.64
Mohr-Coulomb Fit	c (MPa)	12.48
	φ (degree)	42.03

(b)

Figure 6 (a) RMR_{89} histogram distribution for drillhole UGD 189 – 192, where the mean RMR_{89} is 79; (b) Intact strength (after Ooi 2021)

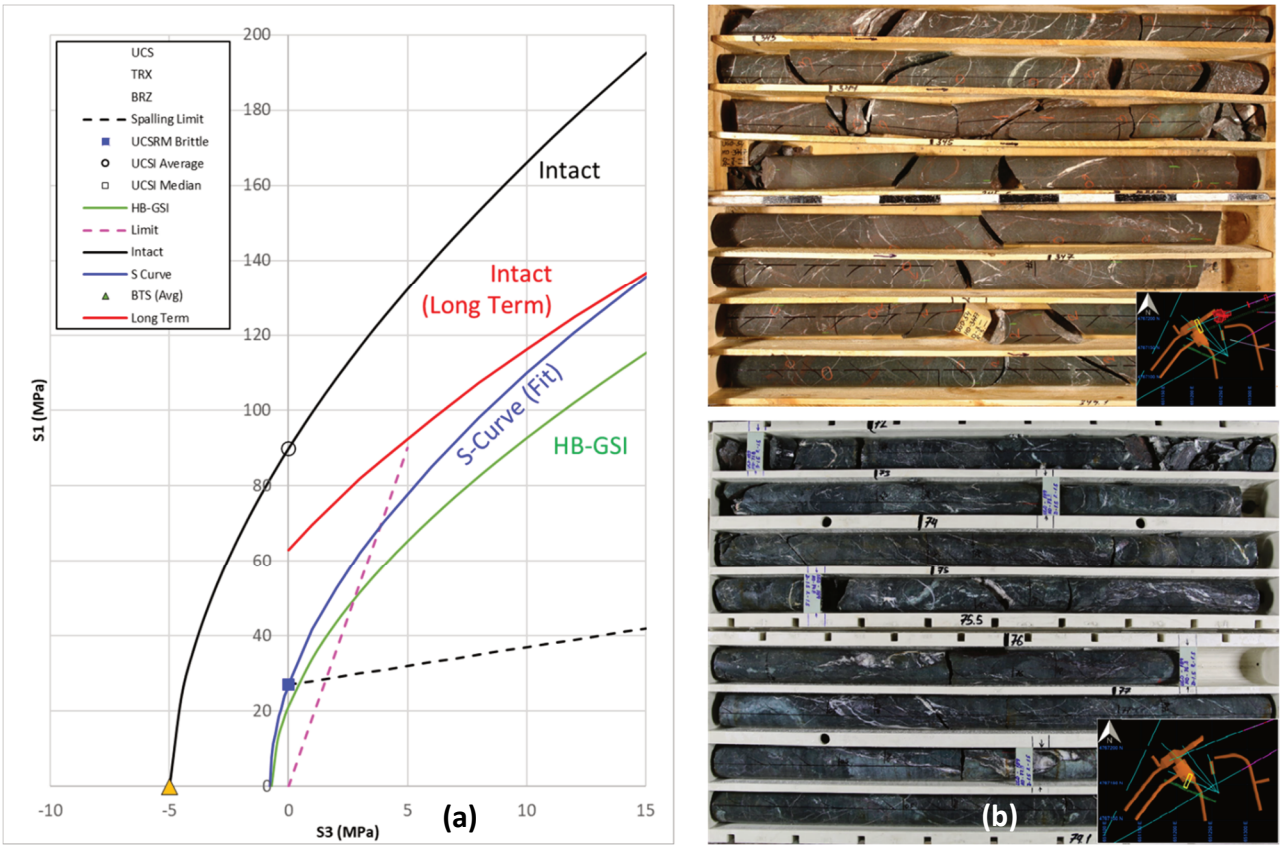

Figure 7 (a) Strength envelopes; (b) Core at the chamber site: strong healed carbonate veining

2.3 In situ principal stress

Due to the tectonic setting near OT, it is not reasonable to use a linear fit to data, by forcing it through zero at zero depth. In the tectonically strained rock mass, the horizontal stresses are elevated by a constant amount over a depth range where the strain is constant and stress relief along faults does not occur. Based on studies in many parts of the world (e.g. the Canadian shield) it is found that there is a stress relieved zone near the surface and a tectonically strain-controlled zone at depth (a depth-independent strain or stress increment added to a gravitational gradient). In between is a transition zone (typically related to macrostructure), where very high strain gradients may be encountered (Martin et al. 2003; Maloney et al. 2016). OT exhibits similar characteristics, where the Contact Fault is the transition zone. Figure 8 illustrates the comparison of the Canadian Shield and Oyu Tolgoi stress regime. The sub-horizontal major principal stress (σ_1) bearing towards 54°, intermediate principal stress (σ_2) is vertical, and minor principal stress (σ_3) is bearing toward 144°. At the production level at 1,300 m, where the raise bores (Figure 9) are predominately located, the σ_1 = 58 MPa, σ_2 = 33 MPa and σ_3 = 27 MPa, and the K ratio of 1.75. Table 2 outlines the stress regime and field gradient.

Table 2 The OT in situ principal stress regime, where the crusher chamber is located at the stress domains 3 at depth of 1,250 m

OT stress domains	Depth range, z (m)	σ_1 (MPa)	σ_2 (MPa)	σ_3 (MPa)	Stress orientation (°)
Domain 1	0–600	0.047z	0.0265z	0.024z	54
Domain 2	600–800	0.071z - 13.95	0.0265z	0.027z - 1.59	Vertical
Domain 3	>800	0.031z + 17.50	0.0265z	0.015z + 7.66	144

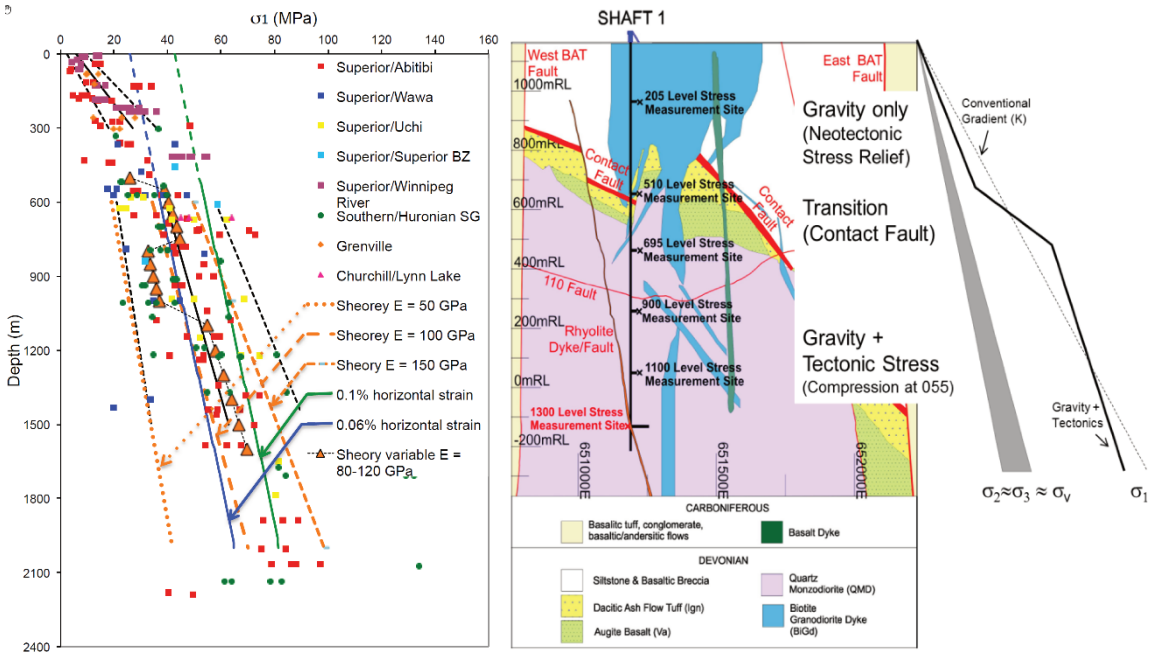

(a) (b)

Figure 8 (a) Stress data from the Canadian Shield (Kaiser et al. 2016); (b) Oyu Tolgoi interpretation stress regime

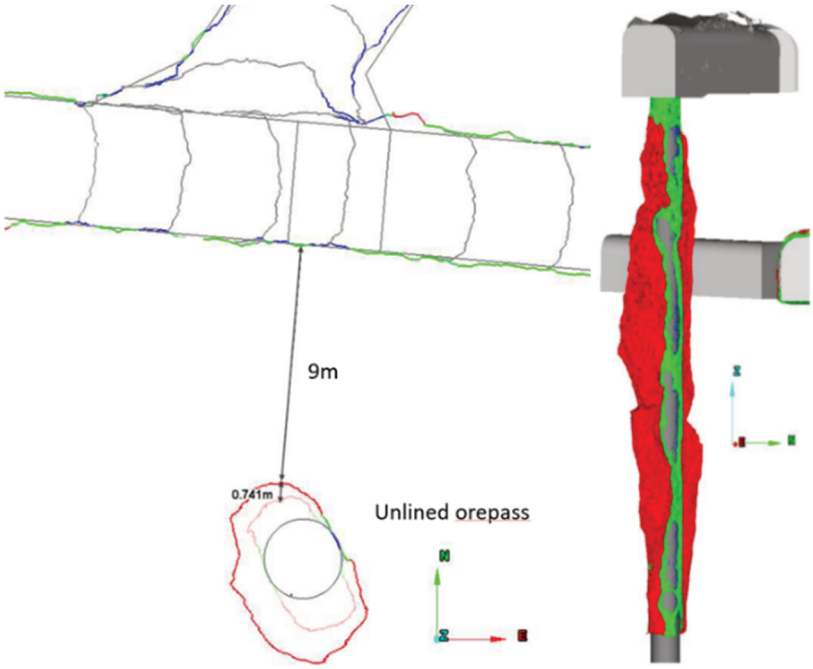

Figure 9 Growth of overbreak of an unlined orepass from GEOSLAM laser scanning, from 3 m diameter to 6 m overbreak, measured in the direction of σ_3 of in situ principal stress, resulted in the diminishing pillar between the raise and tunnel

3 Three-dimensional numerical analysis of chamber response

3.1 Objectives

Numerical modelling with FLAC3D (Itasca Consulting Group (Itasca) 2021) was used to estimate load and deformation 'demands' for use in analytical ground support and reinforcement calculations. In particular, the models were used to calculate depth of damage and convergence during the development of the chamber, and subsequent changes resulting from cave propagation.

A key aspect of the chamber assessment concerns the selection of rock mass strength. Two approaches were assessed as discussed in Section 2.2 namely: HB–GSI and S-Curve. For both strength estimation methods, models were calibrated to observed damage and deformation in (1) tunnels driven sub-perpendicular to S1 near the chamber (2) the current state of the chamber.

3.2 Constitutive model and damage metrics

Accurate estimation of depth of damage and convergence requires careful consideration of geotechnical parameters and selection of a suitable material model for the rock mass. The Itasca Model for Advanced Strain Softening (IMASS) was selected as the model provides good treatment of both the HB–GSI and S-Curve strength estimation methodologies and post-peak behaviour.

IMASS is a strain softening model for simulation of rock mass response to mining (Pierce 2013; Ghazvinian et al. 2020). This model contains a two-stage softening behaviour as shown in Figure Figure 10b. The first residual envelope (blue line) represents the post-peak strength (Figure 10a). At this point, the rock mass is assumed to have undergone fracturing, but the resulting rock fragments are still fully interlocked. Consequently, porosity is considered close to zero. The second residual envelope (green line) represents the ultimate rock mass residual strength at the point of maximum bulking. At this point, the degree of rock fragment interlock is at its minimum, and the porosity is maximised (maximum porosity of 40% is typically assumed). Field observations and bonded block modelling indicates that strength loss (i.e. percentage of peak strength) in the order of more than 25% corelates to substantial damage interpreted as the depth of damage in demand calculations.

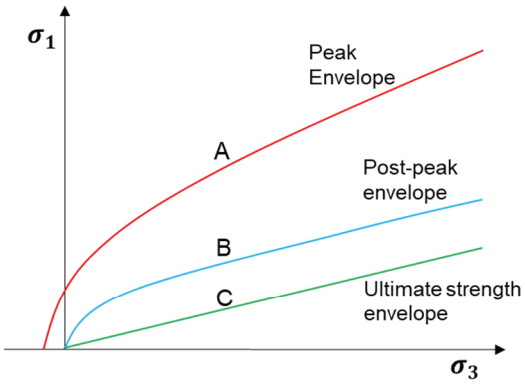

Post-peak:
- High friction angle at low confinement informed by Barton relation.
- Continue to use HB at higher confinement (above brittle-ductile transition).
- Evolves as a function of plastic shear strain via interpolation.

(a)

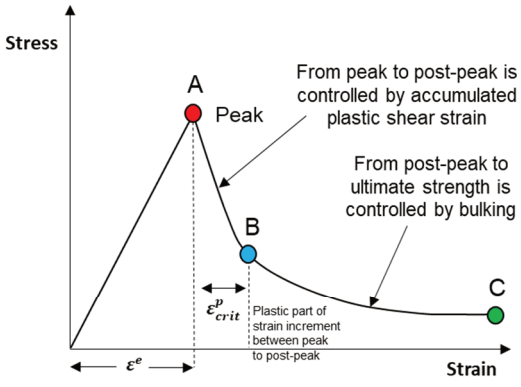

Ultimate strength:
- Lower friction angle at low confinement (close to basic friction angle).
- Continue to use HB at higher confinement (above brittle-ductile transition).
- Evolves as a function of bulking (volumetric strain increment) as informed by Barton relation.

(b)

Figure 10 Yield surfaces and material response for IMASS model

3.3 Chamber sequence and cave geometry and support

The model has 128 stages (Figure 1) including development of the chamber and incremental growth of the three caves. Cave geometry was derived from two sources (Figure 11): preliminary analysis adopted cave shapes directly from CAVESIM utilising the cellular automata for cave propagation (CAP algorithm). The final analysis adopted cave shapes from coupled FLAC3D–CAVESIM models based on the method of Hebert & Sharrock (2018).

Initial models were run using support pressure (based on analytical calculations with encoded load and deformation limits and cut-offs) applied to the sidewalls and backs of the excavation. Later models utilised explicit representation of support (shell elements in FLAC3D 9.0) and reinforcement (Figure 12).

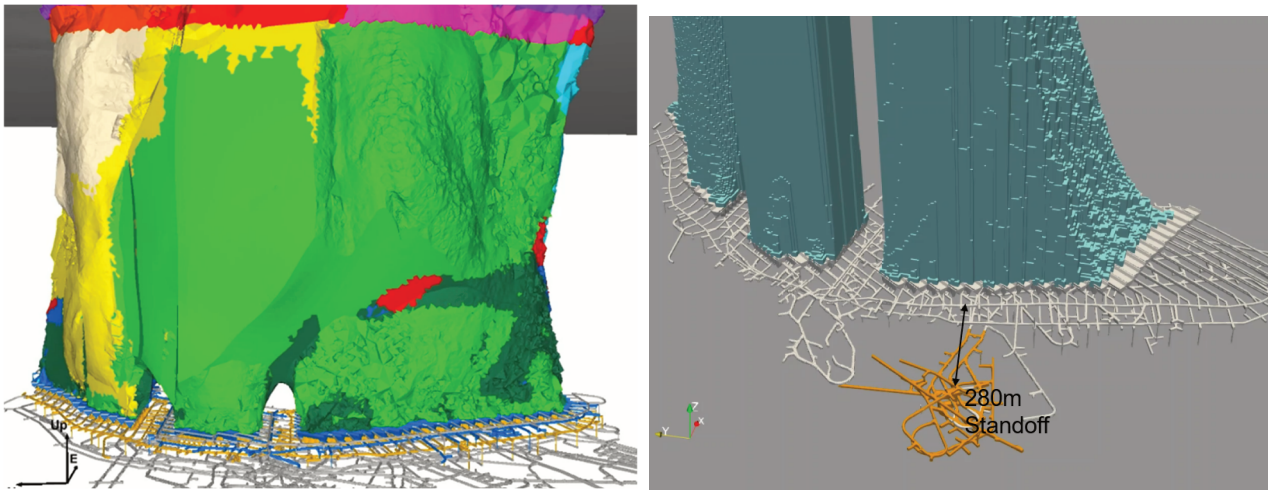

(a) (b)

Figure 11 (a) Coupled FLAC3D–CAVESIM Model incorporating over 500 explicit structures; (b) CAVESIM–CAP algorithm used to generate cave shapes for initial modelling study

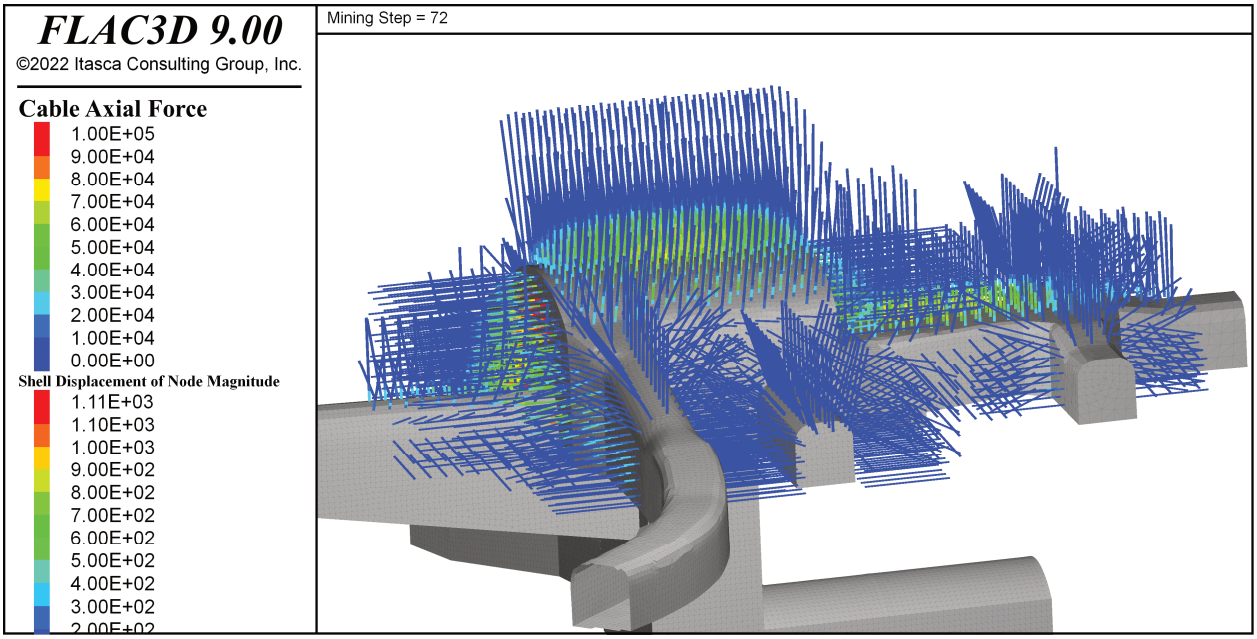

Figure 12 The three-dimensional numerical model of the crusher chamber showing incorporating permanent yielding support, was constructed using the finite difference code FLAC3D (Itasca 2021). Cable force units (N), shell displacement (m)

3.4 Model results

Model results are discussed with reference to the latest observational data and the two strength estimates approaches adopted (i.e. HB–GSI and S-Curve methods).

Depth of damage:

- The HB–GSI and S-Curve methods respectively predict depths of damage of 3 and 1 m. It is noteworthy that the post failure strain softening behaviour of the material is very important and has a significant impact on depth of damage.
- To date no damage has been observed in the chamber back or sidewalls indicating:
  - The HB–GSI method overpredicts damage, in line with Kaiser et el. (2015) and Bewick (2021).
  - Back analysed rock mass strength is higher than GSI method, indicating observed damage has better agreement with the S-Curve strength estimation method.

Convergence: Based on S-Curve properties, deformations due to excavation are less than required for cracking of the FRS, and are assumed to be elastic. Adoption of HB–GSI parameters results in cracking of the FRS which has not been observed to date. Monitoring has been installed for the development of the lower chamber and pillar between the upper and lower chamber.

Stress: The models indicate stress concentrations exists in the back of the upper chamber, and pillars formed between the lower and upper chamber (Figure 13). Minor stress changes including rotation of stress in the chamber back are indicated due to cave interaction. These changes were incorporated into design of the support and reinforcement systems.

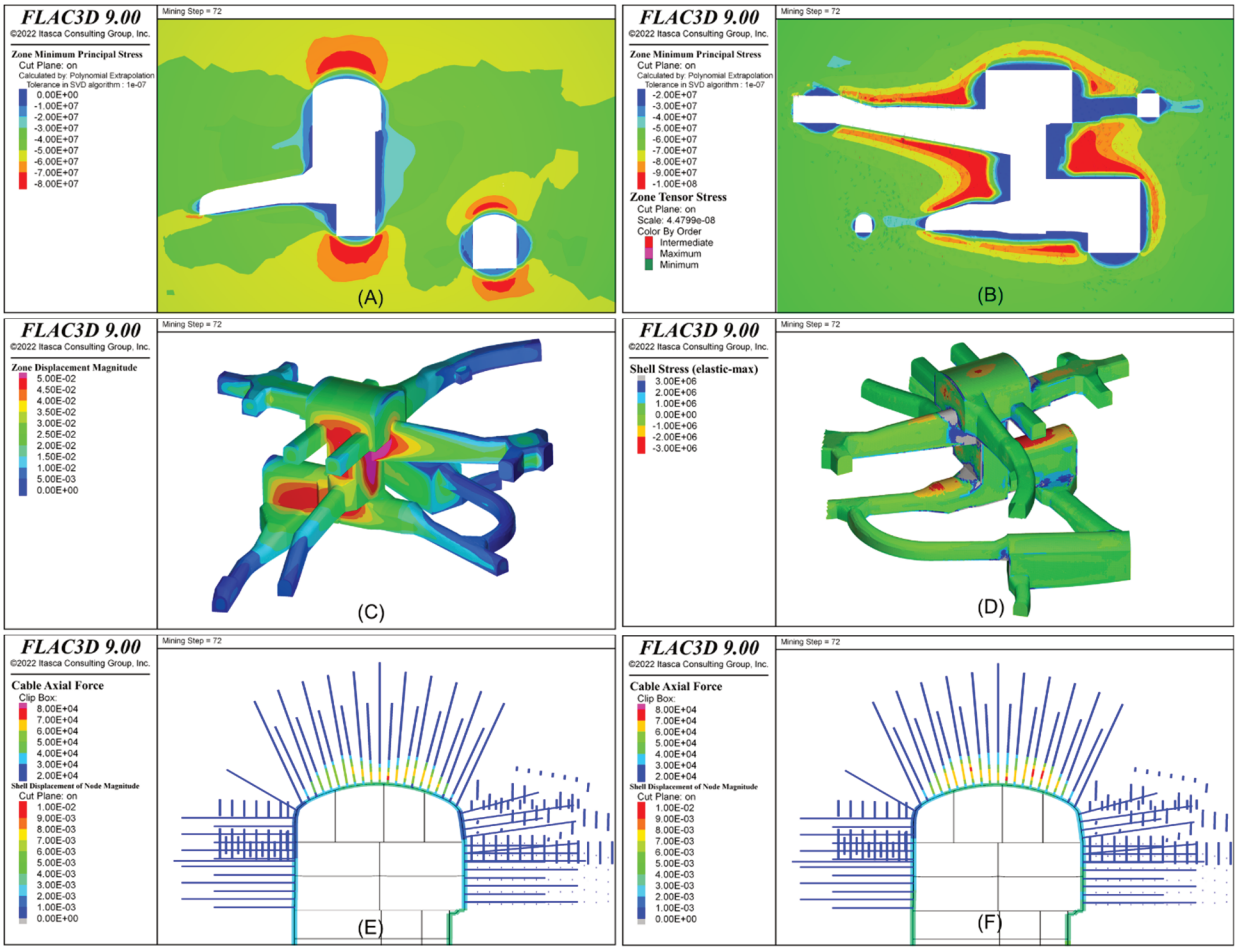

Figure 13 (a, b) Major principal stress (Pa), end of chamber life; (c) Displacement (m); (d) FRS stress (Pa); (e) Cable load (N), after development); (f) Cable load (N), end of life

4 Conclusion

The PC2 crusher chamber is a large excavation located at a depth of 1,300 m in a complex geotechnical environment, in proximity to three large block caves. Determining the ground support and reinforcement for the chamber was an iterative process utilising numerical and analytical methods, accounting for static and dynamic demand, and significant stress redistribution associated with the caves.

Detailed numerical models incorporating a conforming mesh, advanced strain softening model (IMASS), explicit surface support, explicit reinforcement, and explicit structure were used to estimate depth of damage and convergence, for two rock mass strength models: (1) the industry standard Hoek–Brown GSI (HB–GSI) method of Hoek & Brown (2019) and; (2) the brittle (S-Curve) approach of Kaiser et el. (2015) and Bewick (2021).

To date the top chamber has been fully developed and supported, and observations show no damage indicating rock mass strength for high GSI materials is better captured by the S-Curve methodology. This finding agrees with Kaiser et el. (2015) and Bewick (2021).

More case studies are needed to understand the applicability of rock mass strength estimation methods across different rock masses (UCS, GSI, etc) and strain softening assumptions. For now, it is recommended that assessment of chamber excavations utilise both GSI and S-Curve published methodologies for the indicated GSI ranges (GSI <= 65, S-Curve > 65–70).

Acknowledgement

The authors thank Rio Tinto for permission to publish this paper. The authors acknowledge the work of the Oyu Tolgoi site and corporate engineers who collected and analysed the data presented in this paper.

The authors also acknowledge Brett Poulsen, Ian Brunton, and Yoann Hebert of Itasca, who contributed to model construction, benchmarking and validation and technical review.

References

Bewick, RP 2021, 'The strength of massive to moderately jointed rock and its application to cave mining', *Journal of Rock Mechanics and Rock Engineering*, vol. 54, pp. 3629–3661.

Callahan, MF, Keskimaki, KW & Rech, WD 2000, 'A case history of the crusher level development at Henderson', in G Chitombo (ed), *Proceedings of MassMin 2000*, Australasian Institute of Mining and Metallurgy, Melbourne, pp. 307–316.

Campbell, AD, Lilley, CR, Waters, S & Jones, PA 2013, ''Geotechnical analysis and ground support selection for the Ernest Henry crusher chamber', in Y Potvin & B Brady (eds), *Ground Support 2013: Proceedings of the Seventh International Symposium on Ground Support in Mining and Underground Construction*, Australian Centre for Geomechanics, Perth, pp. 437–450, doi.org/10.36487/ACG_rep/1304_29_Campbell

Casten, T, Golden, R, Mulyadi, A & Barber, J 2000, 'Excavation design and ground support of the gyratory crusher installation at the DOZ Mine, PT Freeport Indonesia', in G Chitombo (ed), *Proceedings of MassMin 2000*, Australasian Institute of Mining and Metallurgy, Melbourne, pp. 295–299.

Earl, P 2009, *Ground Control Scheme Design of the West Crusher Complex at Ridgeway Deeps Block Cave*, master's thesis, Curtin University

Ghazvinian, E, Garza-Cruz, T, Bouzeran, L, Fuenzalida, M, Cheng, Z, Cancino, C & Pierce, M 2020, 'Theory and Implementation of the Itasca Constitutive Model for Advanced Strain Softening (IMASS)', in R Castro, F Báez & K, Suzuki (eds), *MassMin 2020: Proceedings of the Eight International Conference and Exhibition on Mass Mining*, University of Chile, Santiago, pp. 451–461.

Hebert, Y & Sharrock, G 2018, 'Three-dimensional simulation of cave initiation, propagation and surface subsidence using a coupled finite difference–cellular automata solution', in Y Potvin & J Jakubec (eds), *Caving 2018: Proceedings of the Fourth International Symposium on Block and Sublevel Caving*, Australian Centre for Geomechanics, Perth, pp. 151–166, doi.org/10.36487/ACG_rep/1815_09_Hebert

Hoek, E 2001, 'Big tunnels in bad rock - 2000 Terzachi lecture', *ASCE Journal of Geotechnical and Geoenvironmental Engineering*, vol. 127, no. 9, pp. 726–740.

Hoek, E 2007, *Practical Rock Engineering*, rocscience.com/learning/hoeks-corner/course-notes-books

Hoek E & Brown ET 2019, 'The Hoek–Brown Failure Criterion and GSI – 2018 edition', *Journal of Rock Mechanics and Geotechnical Engineering*, vol. 11, issue 3, pp. 445–463.

Hormazabal, E, Pereira J, Barindelli, G & Alvarez, R 2014, 'Geomechanical evaluation of large excavations at the New Level Mine - El Teniente', in R Castro (ed), *Caving 2014: Proceedings of the 3rd International Symposium on Block and Sublevel Caving*, University of Chile, Santiago.

Hönisch, K 1988, 'Rock mass modelling for large underground powerhouses', in G Swodoba, *Numerical Methods in Geomechanics*, vol. 3, A.A. Balkema, Rotterdam.

Itasca 2021, FLAC3D (Fast Lagrangian Analysis of Continua), version 7.0, computer software, itascacg.com/software/flac3d, Itasca Consulting Group, Minneapolis.

Kaiser, P, Bewick, R, Amman, F & Pierce, M 2015, *Best Practice in Rock Mass Characterization for Brittle Rock Masses (V2), Rio Tinto Centre for Underground Construction at CEMI*, confidential Rio Tinto report: 12/2015.

Kaiser, PK, Maloney, SM & Yong, S 2016, 'Role of large scale heterogeneities on in-situ stress and induced stress fields', *Proceedings of the 50th U. S. Rock Mechanics/Geomechanics Symposium*, American Rock Mechanics Association, Alexandria.

Maloney, S, Kaiser, PK, & Vorauer, A 2006, 'A re-assessment of in situ stresses in the Canadian Shield', *Proceedings of Golden Rocks 2006*: *The 41st U.S. Symposium on Rock Mechanics*, American Rock Mechanics Association, Alexandria

Martin, CD, Kaiser, PK, & Christiansson, R 2003, 'Stress, instability and design of underground excavations', *International Journal of Rock Mechanics and Mining Sciences*, vol. 40, no. 7–8, pp. 1027–1047, doi.org/10.7939/R3H41JM6V

Ooi, J 2021, *Preliminary Assessment of Rock Mass Characterisation for Primary Crusher Chamber 2 Complex,* document ID: T&IP-OBK-2021-27, confidential Rio Tinto report.

Ooi, J, Watt, G & Grobler, H 2022, 'Raisebore stability and support at deep depth and highly defected rock mass condition: Oyu Tolgoi case study', in Y Potvin (ed), *Caving 2022: Proceedings of Fifth International Conference on Block and Sublevel Caving*, Australian Centre for Geomechanics, Perth, pp. 885–900.

Pierce, M 2013, 'Numerical modeling of rock mass weakening, bulking and softening associated with cave mining', *ARMA e-Newsletter*, spring 2013, issue 9, www.armarocks.org

Player, J, Thompson, AG & Villaescusa, E 2008, 'Dynamic testing of reinforcement system', in TR Stacey & D Malan (ed), *Proceedings of the 6th International Symposium on Ground Support in Mining and Civil Engineering Construction* The South African Institute of Mining and Metallurgy, Johannesburg, pp. 581–595.

Talu, MS & Wilson, AD 2004, 'Innovative mining method and related support systems and quality assurance for a large underground crusher excavation: De Beers Finsch Mine, South Africa', *Proceedings of Massmin 2004*, Instituto de Ingenieros de Chile, Santiago.